

# Bayesian Calibration of the Intelligent Driver Model

Chengyuan Zhang, *Student Member, IEEE*, and Lijun Sun, *Senior Member, IEEE*

**Abstract**—Accurate calibration of car-following models is essential for investigating microscopic human driving behaviors. This work proposes a memory-augmented Bayesian calibration approach, which leverages the Bayesian inference and stochastic processes (i.e., Gaussian processes) to calibrate an unbiased car-following model while extracting the serial correlations of residual. This calibration approach is applied to the intelligent driver model (IDM) and develops a novel model named MA-IDM. To evaluate the effectiveness of the developed approach, three models with different hierarchies (i.e., pooled, hierarchical, and unpooled) are tested. Experiments demonstrate that the MA-IDM can estimate the noise level of unrelated errors by decoupling the serial correlation of residuals. Furthermore, a stochastic simulation method is also developed based on our Bayesian calibration approach, which can obtain unbiased posterior motion states and generate anthropomorphic driving behaviors. Simulation results indicate that the MA-IDM outperforms Bayesian IDM in simulation accuracy and uncertainty quantification. With this Bayesian approach, we can generate enormous but nonidentical driving behaviors by sampling from the posteriors, which can help develop a realistic traffic simulator.

**Index Terms**—car-following, serial correlation, Bayesian inference, hierarchical model, Gaussian processes

## I. INTRODUCTION

Microscopic car-following models are powerful tools to study and simulate human driving behaviors in traffic flows at the trajectory level. They reveal the mechanisms of complex interactions between a subject vehicle and its leading vehicle. These interactions are the essential factors that affect the dynamics of traffic flow and create diverse macroscopic traffic phenomena. However, no model is perfect [1], and car-following models are no exception. Experiences indicate that we can never calibrate a zero-error model that perfectly fits the data [2]. Nevertheless, some car-following models are still valid, with which one can adopt various calibrations (or parameter identification) methods to approximate reality to different extents. Given that the performance and fidelity of microscopic car-following models heavily depend on accurate calibration, improving the reliability of calibration methods is a critical research question.

In recent studies, probabilistic calibration methods have become an emerging and promising approach with a solid statistical foundation. There are essentially two probabilistic

approaches for model calibration. The first approach is maximum likelihood estimation (MLE): we often solve MLE as an optimization problem and finally obtain a point estimate for model parameters; see e.g., [3]. The second approach is Bayesian inference, which allows us to exploit the full posterior distribution for model parameters through Markov chain Monte Carlo (MCMC); see e.g., [4], [5]. In general, the Bayesian inference approach is advantageous in two aspects: (1) we can perform uncertainty quantification based on the full posterior distribution. This is particularly important for a simulation model as we are often interested in the distribution and uncertainty of the simulation results. (2) Bayesian inference offers a hierarchical modeling scheme that allows us to learn parameter distributions at both population and individual levels. A unique advantage of the Bayesian hierarchical model is that it allows us to learn parameters for each individual driver/sample/trajectory, while the population distribution will prevent overfitting by imposing certain dependencies on the parameters. This is particularly important for calibrating car-following models since samples are often short trajectories collected from a large number of drivers with diverse vehicle configurations/dynamics. Considering the substantial differences in personal driving styles and vehicle configurations/dynamics, it is critical to learn the population distribution that can generalize the parameter distribution from short trajectory data. In addition, the learned population distribution can help create diverse driving behaviors to create more realistic simulations with driver heterogeneity. Note that in the following of this paper we refer to “driver behavior” as the characteristics resulting from both the driver and the vehicle.

A fundamental question in performing probabilistic calibration is how to define the probabilistic model and data generation process. Most existing car-following models seek parsimonious structures by simply taking observations from the most recent (i.e., only one) step as input to generate acceleration/speed as output for the current step. However, given the physical inertia and delay in reaction, we should expect the output acceleration/speed to be correlated with and determined by multiple steps of past observations [6]. For instance, Wang et al. [6] show that the best performed deep learning model essentially takes states/observations from the most recent  $\sim 10$  sec as input. As a result, a parsimonious car-following model that only takes one-step past observation/input will inevitably show temporally correlated residuals. Nevertheless, most existing probabilistic calibration methods are developed based on a simple assumption—the residuals are independent and identically distributed (i.i.d.), and as a result, ignoring the autocorrelation in the residuals will lead to biased calibration [7], [8]. For example, Fig. 1 shows the residual process in acceleration ( $a$ ), speed ( $v$ ), and gap ( $s$ ) when calibrating an IDM model with i.i.d. noise, and we can clearly see that the

(Corresponding author: Lijun Sun)

C. Zhang and L. Sun are with the Department of Civil Engineering, McGill University, Montreal, QC H3A 0C3, Canada. E-mail: enzocy@gmail.com (C. Zhang), lijun.sun@mcgill.ca (L. Sun).

The authors would like to thank the McGill Engineering Doctoral Awards (MEDA), the Institute for Data Valorisation (IVADO), the Interuniversity Research Centre on Enterprise Networks, Logistics and Transportation (CIRRELT), Fonds de recherche du Québec – Nature et technologies (FRQNT), and the Natural Sciences and Engineering Research Council (NSERC) of Canada for providing scholarships and funding to support this study.

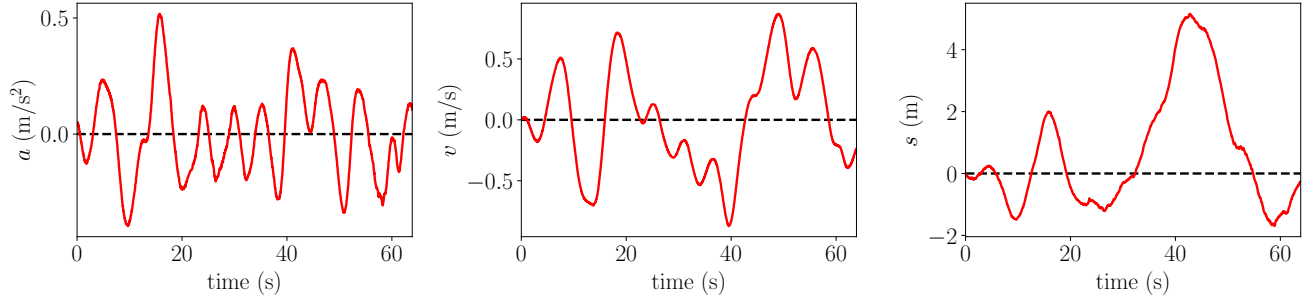


Fig. 1. The residual trends of the calibrated IDM have a strong serial correlation. The ground truth data refer to the unpooled model in Fig. 8.

residuals have strong autocorrelation. To address the serial correlation problem, two classes of methods are developed in the literature. One approach is to directly process the time series data to eliminate serial correlations. For instance, Hoogendoorn and Hoogendoorn [3] adopted a difference transformation (see [9]) to eliminate the serial correlation. However, they used empirical correlation coefficients to perform the transformation instead of jointly learning the IDM parameters and the correlations. Another approach is to explicitly model the serial correlations (e.g., by stochastic processes). For example, Treiber and Kesting [10] introduced Wiener processes to model the temporal correlation of residuals.

In this paper, we propose a novel probabilistic calibration approach that leverages the advantages of Bayesian methods and the power of stochastic processes to calibrate the car-following model unbiasedly. We apply this approach to calibrate the IDM and develop a memory-augmented Bayesian IDM (MA-IDM), which models the serially-correlated residuals as zero-mean Gaussian processes (GP). Taking advantage of the Bayesian methods, we can jointly learn the model parameters and the GP hyperparameters by MCMC. In this work, the MA-IDM is presented in three forms, i.e., pooled model, hierarchical model, and unpooled model. We conduct numerical experiments on the Highway Drone (HighD) Dataset [11], and the results demonstrate that our hierarchical model not only learns disparate driving styles at the population level but also depicts various driving behaviors at the individual level. Additionally, a stochastic simulation method is developed to obtain the posterior motion states in terms of acceleration, speed, and location. In stochastic simulations, one can generate enormous but nonidentical sets of model parameters from the learned posterior distributions, which help characterize anthropomorphic driving behaviors.

The overall contributions of this work are threefold:

- 1) We develop a novel Bayesian calibration approach to learn unbiased parameters and their full posterior distribution. We introduce GP to characterize the autocorrelation in residuals. This approach is applied to calibrate IDM, and results in a novel car-following model, i.e., the MA-IDM.
- 2) We implement the MA-IDM with three hierarchies. Especially with a hierarchical MA-IDM, one can obtain diverse driving styles at the population level and disparate

driving behaviors at the individual level by sampling from the posterior distributions of the well-calibrated hierarchical model. Therefore, we can generate enormous drivers with heterogeneous driving behaviors/styles governed by the same population distribution. Therefore, our model can help create simulations with driver/car heterogeneity.

- 3) We introduce an unbiased stochastic simulator, which is inspired by the corresponding generative process of our Bayesian calibration approach. As a result, the simulator can produce more realistic results than those with homogeneous parameters or random parameters.

The structure of the remaining contents is organized as follows. First, Section II introduces related literature about calibrating car-following models and modeling serial correlations. Section III emphasizes some preliminaries and formulates the car-following problem based on IDM. Then in Section IV, we propose a novel Bayesian calibration method and develop several novel car-following models, i.e., the Bayesian-IDM (B-IDM) and the MA-IDM, with different hierarchies. Next, we conduct extensive experiments and simulations, then thoroughly analyze the results in Section V and Section VI. Finally, Section VIII wraps up this work and discusses several potential directions worth further exploration.

## II. RELATED WORK

### A. Car-Following Model Calibration

The proper choice of key parameters in a car-following model can help depict and replicate complex driving behaviors. As in most cases we never know the values of these parameters, we often collect observable measurements from field car-following data in diverse scenarios and fit the model to the observed data by adjusting the parameters to optimize certain objective functions. The overall process is known as calibration [12]. We refer readers to [2] about calibration of car-following models.

Various calibration methods have been studied in the literature. The genetic algorithm (GA) is one of the most typical and traditional tools as a heuristic evolutionary algorithm [2], [13]. For instance, Punzo et al. [2] conducted extensive experiments to study 29 goodness-of-fit functions (GoF) with the combinations from 3 measures of performance (MoP) and provided systematic guidelines on GA-based calibration. However, GA is sensitive to different choices of GoF and MoP; it is not only computationally expensive but also requires

extensive efforts to search for the best combination of GoF and MoP. Besides, the best combination of one dataset may not be suitable for another. Maximum likelihood (MLE) is a powerful approach. Hoogendoorn et al. [3], [14] first proposed to calibrate car-following models based on MLE. Treiber and Kesting [7] thoroughly investigated the MLE approach on the calibration and validation. MLE seeks to estimate a single “best” value of an unknown quantity, which relies on optimization algorithms. The Bayesian method, as an alternative approach, aims to estimate the distribution of an unknown quantity (i.e., posterior), and often relies on sampling-based algorithms. Rahman et al. [4] calibrated car-following models based on a Bayesian approach. The experiments showed that the Bayesian approach provided much better results than the deterministic optimization algorithm. With the Bayesian approach, Abodo et al. [5] developed a hierarchical model to calibrate Intelligent Driver Model (IDM), which has also achieved promising results.

### B. Serial Correlation Modeling

Regression plays a vital role in model calibration. In the literature, many regression models are developed heavily based on an assumption—the residuals are i.i.d. random variables. However, time series are successive observations with serial correlations, which violates this i.i.d. assumption. For instance, the i.i.d. assumption in the least squares regression methods was challenged by Durbin and Watson [15], in which they tested the errors for independence. Here, we argue that the calibration methods based on i.i.d. assumption would result in biased parameter identification. Generally, as mentioned in [12], the observations are usually regarded as the *true process* with an i.i.d. *observation error*; while in calibration methods, observations are modeled as the combination of a *calibrated model* and an independent *model inadequacy function* with an i.i.d. *observation error*. In calibrations involving time series data, the *model inadequacy function* is mainly used to capture the serial correlations.

There are generally two ways to consider the *model inadequacy* part by investigating the serial correlations: (1) by directly processing the nonstationary data and eliminating serial correlations, such that one can safely ignore the *model inadequacy function* and obtain stationary time series; or (2) by explicitly modeling the serial correlations based on specific *model inadequacy functions*. For instance, Hoogendoorn [3] performed a differencing transformation to eliminate serial correlations, which then showed no significant difference between autocorrelation coefficients and zeros in the previously mentioned Durbin–Watson test [15]. However, the information conveyed by the serial correlations is directly discarded, which prevents us from modeling the generative processes of observations. Another way is to explicitly develop the formation of serial correlations based on further assumptions. For example, state-space models (e.g., Kalman filter [16]) regard the residual trends as a filtering problem based on Markovian assumptions. Dynamic regression models leverage linear regression and autoregressive integrated moving average (ARIMA) model into a single powerful regression model for forecasting time series

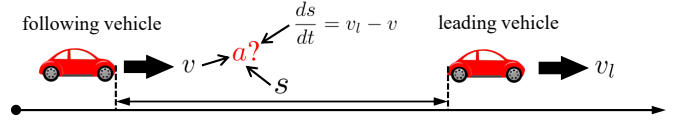


Fig. 2. Physical settings of a car-following scenario.

data [17]. Stochastic processes (e.g., Gaussian processes [18]) are also helpful tools for analyzing time series, which assume time series as manifestations of stochastic processes. These assumptions benefit the methods by deriving concise solutions but constraining some capability. For the main scope of this paper, i.e., calibration and simulation of car-following models, we use Gaussian processes to model the serially correlated residuals (i.e., for the *model inadequacy* part). Gaussian process provides a solid statistical solution to learn unbiased model parameters, and more importantly, it allows us to understand the temporal effect in driving behavior through the lengthscale hyperparameters  $l$ , which partially explains the memory effect of human driving behaviors.

## III. PRELIMINARIES AND PROBLEM FORMULATION

### A. IDM and Probabilistic IDM

The traditional IDM [19] is a continuous nonlinear function  $f : \mathbb{R}^3 \mapsto \mathbb{R}$  which maps the gap, the speed (not velocity)<sup>1</sup>, and the speed difference (approach rate) to acceleration  $a_{\text{IDM}}$  at a certain timestamp. Here, we denote  $s$  as the gap between the following vehicle and the leading vehicle,  $v$  as the speed of the following vehicle, and  $\Delta v = -ds/dt$  (note the minus sign) as the speed difference. The physical meaning of these notations are illustrated in Fig. 2, where  $v_l$  denotes the speed of the leading vehicle. With these notations, IDM is defined as

$$a_{\text{IDM}} = f(s, v, \Delta v) \triangleq \alpha \left( 1 - \left( \frac{v}{v_0} \right)^\delta - \left( \frac{s^*(v, \Delta v)}{s} \right)^2 \right), \quad (1)$$

$$s^*(v, \Delta v) = s_0 + s_1 \sqrt{\frac{v}{v_0}} + vT + \frac{v \Delta v}{2\sqrt{\alpha\beta}}, \quad (2)$$

where,  $v_0, s_0, T, \alpha, \beta$ , and  $\delta$  are model parameters with the following meaning: the desired speed  $v_0$  is the free-flow speed; the jam spacing  $s_0$  denotes a minimum gap distance from the leading vehicle; the safe time headway  $T$  represents the minimum time interval between the following vehicle and the leading vehicle; the acceleration  $\alpha$  and the comfortable braking deceleration  $\beta$  are the maximum vehicle acceleration and the desired deceleration to keep safe, respectively; the exponential coefficient  $\delta$  is a constant, usually set as 4 at default. In IDM, the deceleration is controlled by the desired minimum gap  $s^*$  in Eq. (2), in which we set  $s_1 = 0$  following [19] to obtain a model with interpretable and easily measurable parameters.

To make the notations concise and compact, we define vector  $\theta = [v_0, s_0, T, \alpha, \beta] \in \mathbb{R}^5$  representing the IDM parameters

<sup>1</sup>Note that the term ‘velocity’ represents the directional speed, which is usually denoted as a vector. In the car-following case, motion direction is longitudinal in the vehicle coordinate system at default. Therefore, we use the term ‘speed’ in this paper.

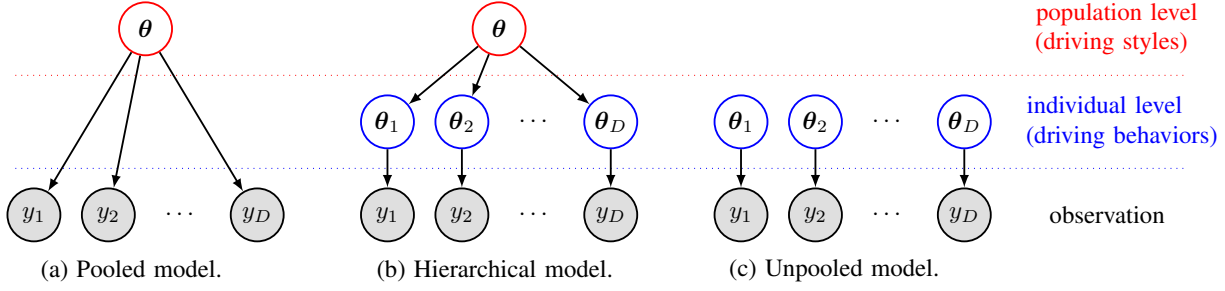


Fig. 3. Pooled model, hierarchical model, and unpooled model.

that we are interested in. For a certain vehicle  $d$ , we have the IDM decisions  $a_{\text{IDM}d}^{(t)} = f(s_d^{(t)}, v_d^{(t)}, \Delta v_d^{(t)})$ , where the subscript  $d$  represents the index for each driver and the superscript  $(t)$  indicates the timestamp. Compactly, we denote the inputs at time  $t$  as a vector  $\mathbf{i}_d^{(t)} = [s_d^{(t)}, v_d^{(t)}, \Delta v_d^{(t)}]$ ,  $\forall t \in \{t_0, \dots, t_0 + (T-1)\Delta t\}$ . Here, we adopt the scheme in [7], [20] with a step of  $\Delta t$  to update vehicle speed and position as following:

$$v^{(t+\Delta t)} = v^{(t)} + a^{(t)} \Delta t, \quad (3a)$$

$$x^{(t+\Delta t)} = x^{(t)} + \frac{v^{(t+\Delta t)} + v^{(t)}}{2} \Delta t. \quad (3b)$$

To this end, one can define a concise function  $\mathcal{F}_{\text{IDM}}$  that updates the following vehicle's speed at  $t + \Delta t$  based on Eq. (3a), written as

$$v_d^{(t+\Delta t)} | \mathbf{i}_d^{(t)}, \boldsymbol{\theta}_d = \mathcal{F}_{\text{IDM}}(\mathbf{i}_d^{(t)}; \boldsymbol{\theta}_d) \triangleq v_d^{(t)} + a_{\text{IDM}d}^{(t)} \Delta t. \quad (4)$$

However, imperfect driving and irregularities in driving behaviors result in erratic components of the driver's action, as stated by Treiber and Kesting [10] in Chapter 12.3.2. It can be modeled by adding to  $a_{\text{IDM}}$  some acceleration noise of standard deviation  $\sigma_\epsilon$ . In such a setting, we consider  $a_{\text{IDM}}$  as a rational behavior model, while the random term as the imperfect driving behaviors that cannot be modeled by IDM. By taking the random term with *i.i.d* assumption into consideration, one can develop a stochastic version of IDM, i.e., the probabilistic IDM [21], [22], written as

$$a_d^{(t)} | \mathbf{i}_d^{(t)}, \boldsymbol{\theta}_d \stackrel{i.i.d.}{\sim} \mathcal{N}(a_{\text{IDM}d}^{(t)}, \sigma_\epsilon^2), \quad (5)$$

where  $a_{\text{IDM}}$  and  $\sigma_\epsilon^2$  represent the mean and variance. Given the dynamic updating in Eq. (4), we have  $v_d^{(t+\Delta t)} = v_d^{(t)} + a_d^{(t)} \Delta t + \epsilon_v$ ,  $\epsilon_v \stackrel{i.i.d.}{\sim} \mathcal{N}(0, (\sigma_\epsilon \Delta t)^2)$ . Thus,

$$v_d^{(t+\Delta t)} | \mathbf{i}_d^{(t)}, \boldsymbol{\theta}_d \stackrel{i.i.d.}{\sim} \mathcal{N}(\mathcal{F}_{\text{IDM}}(\mathbf{i}_d^{(t)}; \boldsymbol{\theta}_d), (\sigma_\epsilon \Delta t)^2). \quad (6)$$

The calibration of car-following model mainly concerns estimating the model parameter  $\boldsymbol{\theta}$  to learn the best mapping from  $\mathbf{i}_d^{(t)}$  to a measure of performance [2], e.g.,  $v_d^{(t+\Delta t)}$  here. Various approaches such as utility-based optimization methods and maximum-likelihood techniques are usually adopted [7].

### B. Pooled, Hierarchical, and Unpooled Model

Here we introduce three different hierarchies of the model, i.e., pooled, hierarchical, and unpooled models, in which hierarchical models are often regarded in terms of “partial

pooling,” compromising between pooled and unpooled models [23]. As shown in Fig. 3, we illustrate the pooling technique and explicitly compare the differences among pooled, hierarchical, and unpooled models. With a pooled model (referred to as complete pooling), all of the drivers  $\forall d \in \{1, \dots, D\}$  is assumed to have the same driving behaviors (characterized by the parameter set  $\boldsymbol{\theta}$ ). While with an unpooled model (referred to as no pooling), each driver  $d$  is assumed to have a completely unrelated parameter set  $\boldsymbol{\theta}_d$ . But with a hierarchical model (referred to as partial pooling), each driver is assumed to have a different parameter set  $\boldsymbol{\theta}_d$ , while the data for all the observed drivers  $d \in \{1, \dots, D\}$  inform the parameter estimates for each driver  $d$ . In general, hierarchical models consider a population model of drivers as the prior for each specific driver. And from this population model perspective, the unpooled model corresponds to infinite population variance, whereas pooled model corresponds to zero population variance.

## IV. BAYESIAN CALIBRATION OF CAR FOLLOWING MODEL

In this section, we develop a novel Bayesian calibration method and apply it to calibrate IDM. Specifically, we present the formulations of four models, i.e., the pooled and the hierarchical models of the B-IDM and the MA-IDM, respectively. The corresponding probabilistic graphical models are shown in Fig. 4.

### A. Pooled and Hierarchical Bayesian IDM (B-IDM)

Firstly, we introduce the form of the pooled B-IDM:  $\forall (t, d) \in \{(t, d)\}_{t=t_0, d=1}^{t_0+(T-1)\Delta t, D}$ , we have

$$\ln(\boldsymbol{\theta}) \sim \mathcal{N}(\boldsymbol{\mu}_0, \boldsymbol{\Sigma}_0) \in \mathbb{R}^5, \quad (7a)$$

$$\ln(\sigma_\epsilon) \sim \mathcal{N}(\mu_\epsilon, \sigma_1) \in \mathbb{R}, \quad (7b)$$

$$v_d^{(t+\Delta t)} | \mathbf{i}_d^{(t)}, \boldsymbol{\theta} \stackrel{i.i.d.}{\sim} \mathcal{N}(\mathcal{F}_{\text{IDM}}(\mathbf{i}_d^{(t)}; \boldsymbol{\theta}), (\sigma_\epsilon \Delta t)^2) \in \mathbb{R}. \quad (7c)$$

In the previous literature [5], some samples that drawn from the Markov chains are unrealistically with negative values. To avoid this, here we assume  $\boldsymbol{\theta}$  and  $\sigma_\epsilon$  are log-normal distributed. With such a setting, one can ensure the corresponding parameters falls in the set of positive real number  $\mathbb{R} = \{x \in \mathbb{R} \mid x > 0\}$ .

However, the pooled model can only capture the general driving styles of a “population driver.” To characterize and model the heterogeneity in driving behavior, one can learn different parameters for each sample of the data, which translates to introducing heterogeneity at the level of the driver

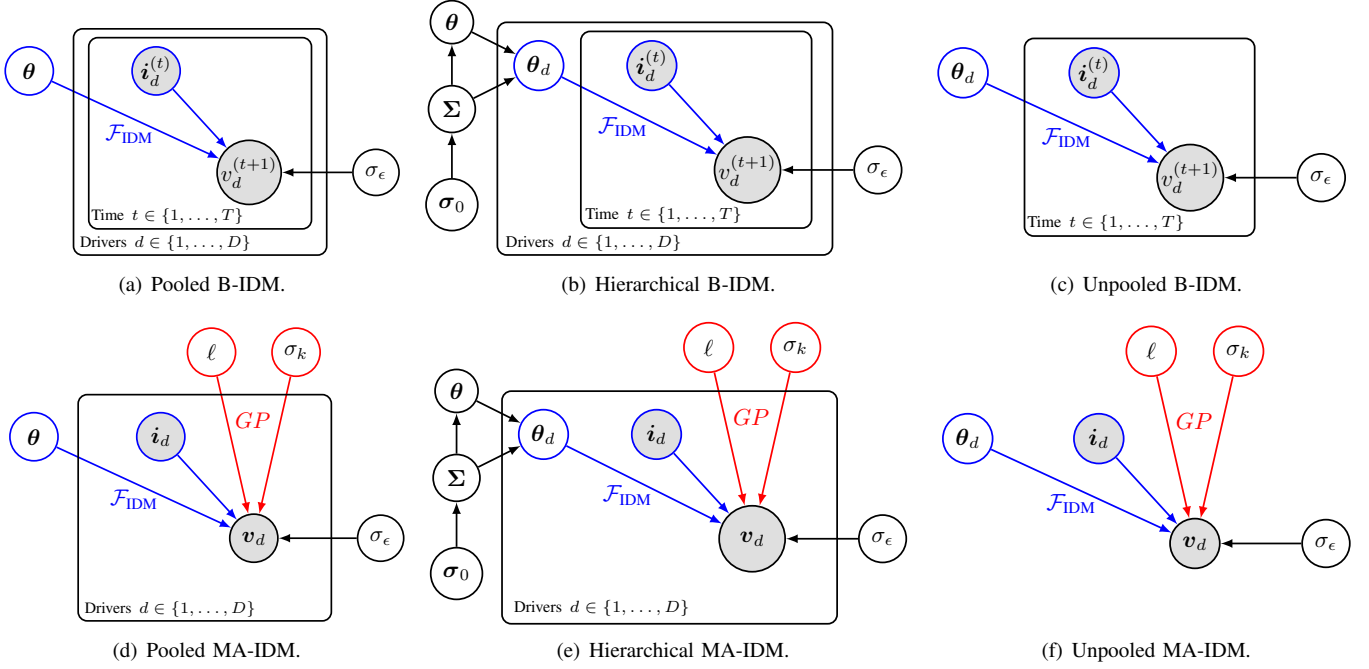


Fig. 4. Probabilistic graphical models.

population [10]. Here we develop a hierarchical B-IDM that explicitly models the general driving behaviors at the population level, then depicts heterogeneous behaviors at the individual level, described as follows:  $\forall (t, d) \in \{(t, d)\}_{t=t_0, d=1}^{t_0+(T-1)\Delta t, D}$ , we have

$$\sigma_0 \sim \text{Exp}(\lambda) \in \mathbb{R}^5, \quad (8a)$$

$$\Sigma \sim \text{LKJCholeskyCov}(\eta, \sigma_0) \in \mathbb{R}^{5 \times 5}, \quad (8b)$$

$$\ln(\theta) \sim \mathcal{N}(\mu_0, \Sigma) \in \mathbb{R}^5, \quad (8c)$$

$$\ln(\theta_d) \sim \mathcal{N}(\ln(\theta), \Sigma) \in \mathbb{R}^5, \quad (8d)$$

$$\ln(\sigma_\epsilon) \sim \mathcal{N}(\mu_\epsilon, \sigma_1) \in \mathbb{R}, \quad (8e)$$

$$v_d^{(t+\Delta t)} | i_d^{(t)}, \theta_d \stackrel{i.i.d.}{\sim} \mathcal{N}(\mathcal{F}_{\text{IDM}}(i_d^{(t)}; \theta_d), (\sigma_\epsilon \Delta t)^2) \in \mathbb{R}. \quad (8f)$$

where LKJ stands for the LKJ distribution developed by Lewandowski, Kurowicka, and Joe [24]. And LKJCholeskyCov is a distribution over Cholesky decomposed covariance matrices, such that the underlying correlation matrices follow an LKJ distribution and the standard deviations follow an exponential distribution, as specified by PyMC [25]. In practice, LKJCholeskyCov distribution is a more robust prior for covariance matrix than the inverse-Wishart distribution [26].

### B. Pooled and Hierarchical Memory-Augmented IDM (MA-IDM)

For daily driving tasks, temporally-consistent inertia of actions/motions is one of the vital driving profiles for human drivers. This phenomenon is termed as *driving persistence* in [10]. For instance, if drivers slam on their brakes too hard at a certain timestamp, they will likely persist in a vast deceleration in the next seconds. However, in most stochastic models, as well as B-IDM introduced above, the persistence of the acceleration noise is ignored, and its time dependence is wrongly modeled

by white noise, such as in Eq. (5). To make this point clear, we reformulate Eq. (5) as

$$a_d^{(t)} = a_{\text{IDM}d}^{(t)} + \epsilon_t, \quad \epsilon_t \stackrel{i.i.d.}{\sim} \mathcal{N}(0, \sigma_\epsilon^2). \quad (9)$$

However, the developed models and the calibrated parameters are only valid if the residuals conform to the i.i.d. assumption, and the temporal correlation in residuals leads to the biased estimation of model parameters. In the following, we will derive an unbiased Bayesian model in the pooled and hierarchical form by modeling the time-dependent stochastic residual term with Gaussian processes.

Given the nature of time-series autocorrelation, we model the  $\epsilon_t$  in Eq. (9) by Gaussian processes, such that

$$a_d^{(t)} = a_{\text{IDM}d}^{(t)} + a_{\text{GP}d}^{(t)} + \epsilon \quad (10)$$

with  $\epsilon$  as time-independent i.i.d. noise, and  $a_{\text{GP}d}^{(t)} \sim \mathcal{GP}(0, k(t, t'))$ , where  $k$  is the kernel function. Specifically, if we evaluate the continuous function at several discrete timestamps  $t = t_0, \dots, t_0 + (T-1)\Delta t$  with step  $\Delta t$  to obtain  $\mathbf{a}_{\text{GP}d} = \{a_{\text{GP}d}^{(t)}\}$ , from the definition of Gaussian processes, the prior distribution  $p(\mathbf{a}_{\text{GP}d})$  is usually set as a zero-mean Gaussian with a Gram matrix  $\mathbf{K}$  being the covariance matrix, written as

$$\mathbf{a}_{\text{GP}d} \sim \mathcal{N}(\mathbf{0}, \mathbf{K}) \in \mathbb{R}^T, \quad (11)$$

where  $\mathbf{K} \in \mathbb{R}^{T \times T}$  is the Gram matrix

$$\mathbf{K} = \begin{bmatrix} k(\Delta t, \Delta t) & \cdots & k(\Delta t, T\Delta t) \\ \vdots & \ddots & \vdots \\ k(T\Delta t, \Delta t) & \cdots & k(T\Delta t, T\Delta t) \end{bmatrix} \in \mathbb{R}^{T \times T}. \quad (12)$$

Here we specify that  $k$  is the squared exponential kernel  $k(t, t') = \sigma_k^2 \exp\left(-\frac{(t-t')^2}{2\ell^2}\right)$  with  $\ell$  being the lengthscale and

$\sigma_k^2$  being the noise variance. Notice that we reformulated  $\mathbf{K}$  for concise notations with the property  $k(t_0, t) \equiv k(t_0 + \Delta t, t + \Delta t) \equiv k(\Delta t, t - t_0 + \Delta t)$ .

In a compact form, by combining  $\mathbf{a}_{\text{IDM}d}$ ,  $\mathbf{a}_{\text{GP}d}$  and  $\epsilon$ , we have

$$\mathbf{a}_d | \mathbf{i}_d, \boldsymbol{\theta}_d \sim \mathcal{N}(\mathbf{a}_{\text{IDM}d}, \mathbf{K} + \sigma_\epsilon^2 \mathbf{I}) \in \mathbb{R}^T, \quad (13)$$

where  $\mathbf{I} \in \mathbb{R}^{T \times T}$ .

Upon the above discussion, we absorb the  $\mathbf{a}_d$  from Eq. (13) into the B-IDM, one can obtain the pooled and the hierarchical MA-IDM which will be discussed in the following.

For the pooled MA-IDM,  $\forall d \in \{1, \dots, D\}$ , we have

$$\ln(\boldsymbol{\theta}) \sim \mathcal{N}(\boldsymbol{\mu}_0, \boldsymbol{\Sigma}_0) \in \mathbb{R}^5, \quad (14a)$$

$$\ln(\sigma_\epsilon) \sim \mathcal{N}(\mu_\epsilon, \sigma_1) \in \mathbb{R}, \quad (14b)$$

$$\ln(\sigma_k) \sim \mathcal{N}(\mu_k, \sigma_2) \in \mathbb{R}, \quad (14c)$$

$$\ln(\ell) \sim \mathcal{N}(\mu_\ell, \sigma_\ell) \in \mathbb{R}, \quad (14d)$$

$$v_d | \mathbf{i}_d, \boldsymbol{\theta} \sim \mathcal{N}(\mathcal{F}_{\text{IDM}}(\mathbf{i}_d; \boldsymbol{\theta}), (\mathbf{K} + \sigma_\epsilon^2 \mathbf{I}) \Delta t^2) \in \mathbb{R}^T. \quad (14e)$$

Note that different from Eq. (7c), we have a multivariate normal distribution in Eq. (14e).

Similarly, we can develop the hierarchical MA-IDM as

$$\sigma_0 \sim \text{Exp}(\lambda) \in \mathbb{R}^5, \quad (15a)$$

$$\boldsymbol{\Sigma} \sim \text{LKJCholeskyCov}(\eta, \boldsymbol{\sigma}_0) \in \mathbb{R}^{5 \times 5}, \quad (15b)$$

$$\ln(\boldsymbol{\theta}) \sim \mathcal{N}(\boldsymbol{\mu}_0, \boldsymbol{\Sigma}) \in \mathbb{R}^5, \quad (15c)$$

$$\ln(\boldsymbol{\theta}_d) \sim \mathcal{N}(\ln(\boldsymbol{\theta}), \boldsymbol{\Sigma}) \in \mathbb{R}^5, \quad (15d)$$

$$\ln(\sigma_\epsilon) \sim \mathcal{N}(\mu_\epsilon, \sigma_1) \in \mathbb{R}, \quad (15e)$$

$$\ln(\sigma_k) \sim \mathcal{N}(\mu_k, \sigma_2) \in \mathbb{R}, \quad (15f)$$

$$\ln(\ell) \sim \mathcal{N}(\mu_\ell, \sigma_\ell) \in \mathbb{R}, \quad (15g)$$

$$v_d | \mathbf{i}_d, \boldsymbol{\theta}_d \stackrel{i.i.d.}{\sim} \mathcal{N}(\mathcal{F}_{\text{IDM}}(\mathbf{i}_d; \boldsymbol{\theta}_d), (\mathbf{K} + \sigma_\epsilon^2 \mathbf{I}) \Delta t^2) \in \mathbb{R}^T. \quad (15h)$$

## V. EXPERIMENTS

In this section, we access the performance of our proposed car-following models by calibrating on naturalistic human-driving car-following data.

### A. Experimental Settings

1) *Dataset*: The behavior of car-following models can be affected and contaminated by the noise in empirical data [27]. Therefore, selecting an appropriate dataset can keep the model performances away from data quality impact at the most while relieving us from the redundant work of filtering the data noise. In this paper, we use the HighD dataset [11]—a high-resolution trajectory data collected using drones. Compared with the widely-used NGSIM dataset [28], HighD benefits from advanced computer vision techniques and more reliable data-capture methods.

The HighD dataset has 60 video recordings, logged with the sampling frequency of 25 Hz on several German highway sections with a length of 420 m. In each recording, the trajectories, velocities, and accelerations of two types of vehicles (car and truck) are measured and estimated. We follow the same data processing procedures as in [29] to transform the data into a new coordinate system.

2) *Car-Following Data Extraction*: According to [30], long trajectories are preferred for robust estimation of IDM parameters. Thus, we first filter out the data with a car-following duration lasting less than a certain threshold  $t_0$  to extract leader-follower pairs. To obtain informative stop-and-go data with frequent interactions, we set  $t_0 = 50$  s. Then we randomly select 8 leader-follower pairs from these interactive data for each type of vehicle, respectively. Fig. 5 shows examples of the trajectories used for model training. It should be noted that here we only consider the heterogeneity of the follower; if interested, readers can also investigate different combinations of more types of vehicles for both the leader and the follower, e.g., as discussed in [31].

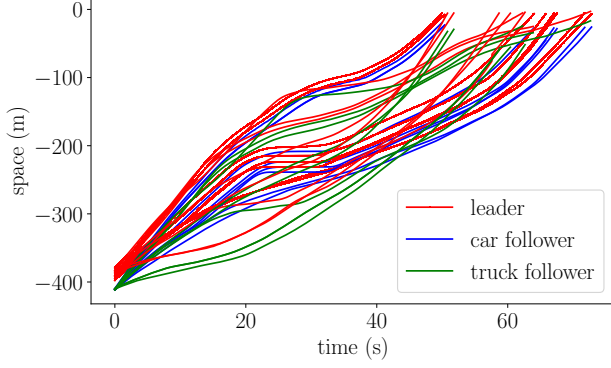
3) *MCMC Settings*: Here we assume that the internal states of each driver are consistent, such that human drivers do not change their driving styles in the region of interest (ROI). In this work, we utilize PyMC [25] to estimate the posterior distributions. Specifically, we adopt one kind of Hamiltonian Monte Carlo (HMC) method, i.e., the No-U-Turn Sampler (NUTS) [32], and we set the burn-in steps as 20000 to make sure the detailed balance condition holds for the Markov chains. The IDM priors are set by mainly following the recommended values  $\boldsymbol{\theta}_{\text{rec}} = [33.3, 2.0, 1.6, 0.73, 1.67]$  in [30], e.g., the population prior  $\boldsymbol{\mu}_0$  are set as  $\ln(\boldsymbol{\theta}_{\text{rec}})$ . As for other hyperparameters, we set  $\lambda = 100$  for the exponential distribution;  $\eta = 2$  for the LKJCholeskyCov distribution; and the hyperparameters for the log-normal distributions of  $\sigma_\epsilon$ ,  $\sigma_k$ , and  $\ell$  are flexible, one can adjust them to ensure that they are positive values falling in reasonable ranges.

4) *Reproducibility*: All codes for reproducing the experiment results reported in this paper will be available at [https://github.com/Chengyuan-Zhang/IDM\\_Bayesian\\_Calibration](https://github.com/Chengyuan-Zhang/IDM_Bayesian_Calibration).

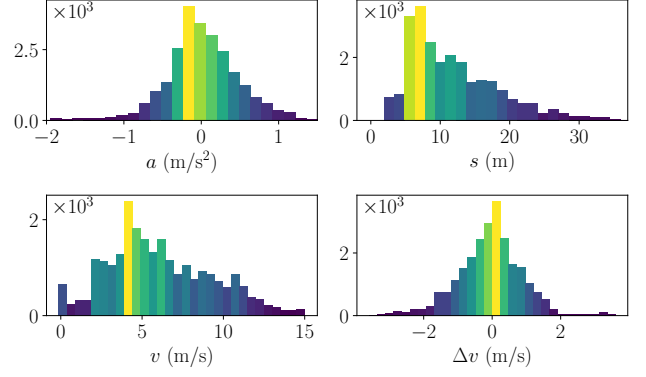
### B. Calibration Results and Analysis

We compare the calibration results of the pooled, hierarchical, and unpooled models for the B-IDM and the MA-IDM in the following. The most straightforward results are the calibrated IDM parameters in the form of posterior distributions, for which we utilized *corner.py* [33] for visualizations. Here we use the hierarchical models as examples to illustrate our results. We visualized the posterior distributions of  $\boldsymbol{\theta}_d$  (i.e., at the individual level) for two drivers in Fig. 6 and Fig. 7, respectively. The posterior distributions of the B-IDM seem pretty similar to that of the MA-IDM. To make it clearer to compare, we summarize the posterior expectations of each parameter in Table I.

1) *Correlation matrices*: From the upper right part of each subfigure in Fig. 6 and Fig. 7, the correlation matrices indicate several strong correlations among IDM parameters. The strong positive correlations exist in the pairs of  $(T, \alpha)$ ,  $(T, \beta)$ , and  $(\alpha, \beta)$ ; while the strong negative correlations exist in the pairs of  $(v_0, s_0)$ ,  $(v_0, \alpha)$ ,  $(s_0, T)$ ,  $(s_0, \alpha)$ , and  $(s_0, \beta)$ . These correlations basically consistent with the results in the literature [7], in which the calibrations were based on the likelihood but not the posterior. Also, the correlation matrices of  $\boldsymbol{\theta}_d$  at the individual level are also consistent by using the hierarchical models and the unpooled models.

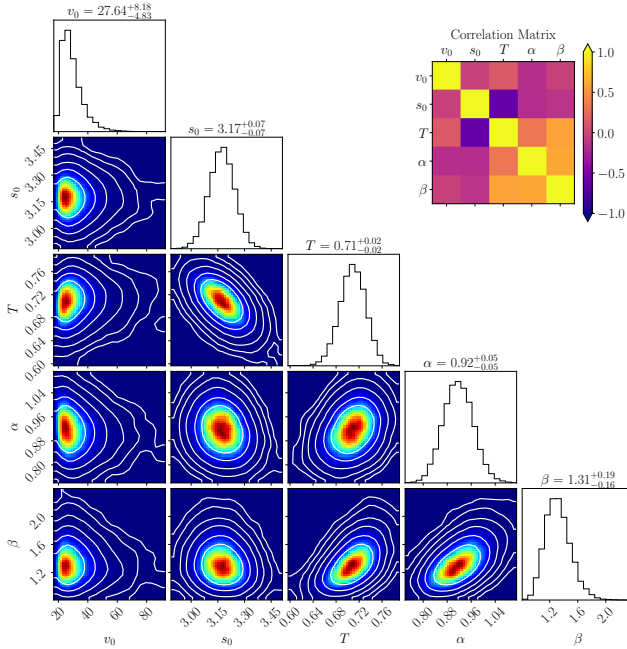


(a) Trajectory visualization.

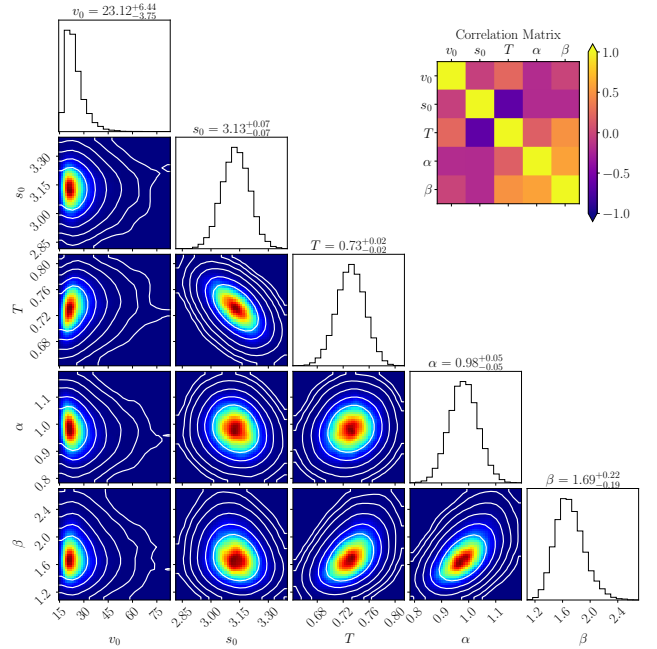


(b) Empirical histogram.

Fig. 5. Visualizations of the 16 selected leader-follower pairs.



(a) Hierarchical B-IDM posteriors of car #355.



(b) Hierarchical MA-IDM posteriors of car #355.

Fig. 6. The posterior distributions and the correlation matrices of the parameters of a car driver #355 in the hierarchical B-IDM and MA-IDM.

2) *Analysis of the calibrated IDM parameters:* We verify that all of the calibrated parameters fall in the recommendation ranges according to [34]. And the calibration results in Table I demonstrate the reliability of our methods to calibrate plausible IDM parameters. In the following, we make some comparisons among several pairs of calibration results.

Firstly, one obvious conclusion is that cars tend to have larger maximum vehicle acceleration  $\alpha$  than trucks. Recall that the  $\alpha$  in Eq. (1) is an amplification coefficient that acts on the entire function. This finding aligns with the truth that trucks are heavier, and truck drivers often use eco-friendly driving strategies to avoid aggressive accelerations.

Secondly, the results of the pooled model indicate the general driving behavior of a ‘population driver,’ i.e., the model learns a set of IDM parameters with a moderate driving policy, which

expects to explain all behaviors in the data. However, as we noticed that human driving behaviors vary from one driver to another because of disparate driving situations, the capability of the pooled model is limited in explaining heterogeneous data. Consequently, the pooled model considers the diversity as errors to compensate for the uncertain behaviors and assign a significant variance  $\sigma_\epsilon^2$  to the residual term. The unpooled model, on the other hand, is an example with smaller residual variance  $\sigma_\epsilon^2$ , since it creates and fits a separable model for each specific driver at the risk of overfitting.

Thirdly, we obtain mostly similar identified parameter values between hierarchical and unpooled models at the individual driver’s level. The results demonstrate the consistency of our proposed models with different hierarchies. Also, it strongly supports the claim that the hierarchical models can simul-

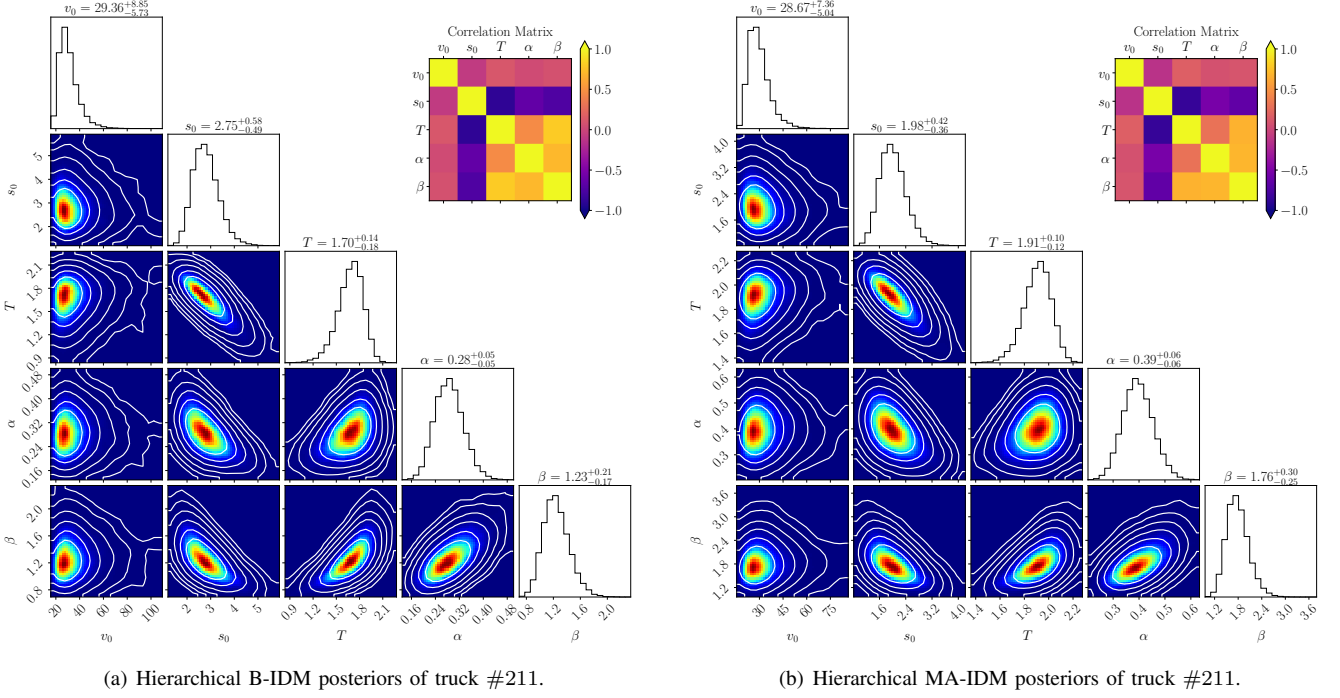


Fig. 7. The posterior distributions and the correlation matrices of the parameters of two representative driver #211 in the hierarchical B-IDM and MA-IDM.

TABLE I  
POSTERIOR EXPECTATIONS OF MODEL PARAMETERS.

	$\theta = [v_0, s_0, T, \alpha, \beta]$	$\sigma_\epsilon$	$\sigma_k$	$\ell$
Pooled B-IDM (car)	[14.552, 2.906, 0.469, 0.622, 1.267]	0.517	/	/
Pooled B-IDM (truck)	[14.844, 5.305, 0.229, 0.568, 1.205]	0.487	/	/
Hierarchical B-IDM (population)	[27.142, 3.647, 0.810, 0.424, 2.065]	0.334	/	/
Hierarchical B-IDM (car #355)	[29.340, 3.173, 0.709, 0.917, 1.319]	0.334	/	/
Hierarchical B-IDM (truck #211)	[31.013, 2.800, 1.680, 0.287, 1.246]	0.334	/	/
Unpooled B-IDM (car #355)	[22.633, 3.190, 0.697, 0.935, 1.211]	0.410	/	/
Unpooled B-IDM (truck #211)	[32.580, 1.467, 2.050, 0.325, 1.555]	0.260	/	/
Pooled MA-IDM (car)	[13.629, 2.579, 0.422, 0.531, 1.754]	0.105	0.250	32.778 (1.311 s)
Pooled MA-IDM (truck)	[14.134, 5.101, 0.275, 0.539, 1.758]	0.102	0.242	37.226 (1.489 s)
Hierarchical MA-IDM (population)	[20.617, 3.672, 0.710, 0.693, 2.657]	0.103	0.212	33.141 (1.326 s)
Hierarchical MA-IDM (car #355)	[24.514, 3.130, 0.732, 0.982, 1.709]	0.103	0.212	33.141 (1.326 s)
Hierarchical MA-IDM (truck #211)	[29.938, 2.013, 1.907, 0.397, 1.788]	0.103	0.212	33.141 (1.326 s)
Unpooled MA-IDM (car #355)	[18.334, 3.182, 0.699, 0.969, 1.400]	0.103	0.164	25.542 (1.022 s)
Unpooled MA-IDM (truck #211)	[27.059, 1.294, 2.086, 0.408, 1.942]	0.102	0.137	32.938 (1.318 s)

\* Recommendation values [19]:  $\theta_{\text{rec}} = [33.3, 2.0, 1.6, 0.73, 1.67]$ .

taneously identify style-specific IDM parameters for diverse drivers.

3) *Analysis of GP parameters:* Recall that the RBF kernel function  $k$  has two essential hyperparameters, the lengthscale  $\ell$  and the noise variance  $\sigma_k^2$ . One can refer to Table I for the identified parameters of the MA-IDM.

First, we focus on analyzing the lengthscale  $\ell$ . Theoretically, for  $f \sim \mathcal{GP}(0, k)$ , the correlation between  $f(x)$  and  $f(y)$  is  $k(x, y)$ , e.g., when  $\|x - y\| = \ell$ , the correlation is  $\exp(-1/2) \approx 0.61$ . In the setting of car-following scenarios,  $\ell$  can be interpreted as an action delay in the stimulus-response mechanism. From the results, we conclude that in our case, the car-following motion delay has: a decent amount of correlation within  $\ell \approx 1.33$  s; and is only slightly dependent within  $2\ell \approx 2.66$  s; but essentially independent

out of  $3\ell \approx 4.00$  s. These results are also consistent with the literature; a driving reaction time of 1.5 seconds was concluded in [35]. Additionally, all pooled, hierarchical, and unpooled models show that truck drivers have longer reaction delays  $\ell$  than car drivers. We also noticed that the unpooled models have smaller  $\ell$  than the pooled models, which is reasonable—the pooled models are less accurate and have to compensate for the uncertainty by increasing  $\ell$  to obtain more likelihood of explaining the data.

Besides, experiments demonstrate that the variance  $\sigma_\epsilon^2$  of the time-independent i.i.d. noise  $\epsilon$  could be decreased at a significance level by introducing GP. One should note that the  $\sigma_\epsilon^2$  of the B-IDM varies as we use disparate models or calibrate on different data. However, we would expect the random i.i.d. noise to be at almost the same level for the same dataset. On the

other side, for the MA-IDM, the  $\sigma_\epsilon^2$  stabilized approximately to  $0.1 \text{ m/s}^2$ , which demonstrates that the errors captured by  $\epsilon$  are i.i.d. In addition, the overall residual noise level (including the parts explained by GP) is significantly decreased, which reflects that the calibrated IDM can better fit the data. Thus, we can identify the effectiveness of the temporally correlated residual modeling in the MA-IDM.

### C. Data Completeness and Parameter Orthogonality

Several questions are worth considering before calibrating the model: What scenarios may the data contain to train a well-calibrated model? There are several parameters in the IDM formulation; are these parameters equally important? Do we need to calibrate all the parameters [30]? The previous literature has reported that parts of the parameters could not be determined directly from the data due to insufficient information [3]. Researchers also developed a reduced IDM that fixes some unimportant parameters [30]. Also, the identifiability of car-following systems is discussed in [36]. We analyze these problems from data completeness and parameter orthogonality perspectives in this part.

Parameter orthogonality of IDM was first discussed in [7], in which the parameter orthogonality is illustrated as “different identifiable driving situations are represented by disparate parameters, ideally one for each situation.” We notice that in Eq. (1) the two parameters  $v_0$  and  $\delta$  are correlated with each other and orthogonal to the remaining parameters in  $\theta$ . Specifically, they are shown in the same term  $(\frac{v}{v_0})^\delta$  but nowhere else. Given a certain  $v$  and a specific quantity of this term, one can find infinite groups of the combination of  $v_0$  and  $\delta$ . Experiments show that if we jointly calibrate  $v_0$  and  $\delta$ , they would both converge to their priors. Therefore, for the sake of avoiding fractional exponential order and numerically unstable issues, we followed the conventional settings and fix  $\delta = 4$  to obtain a parameter orthogonal model.

Then we verify the completeness of the car-following data used in this work. The IDM parameters need to be learned from corresponding data collected in specific scenarios. For instance,  $v_0$  is learned from the free-flow data;  $s_0$  and  $T$  are learned from the car-following data;  $\alpha$  is learned from the freely accelerating data, and  $\beta$  is learned from the approaching (with braking) data. However, since we only selected the interactive stop-and-go data, we don’t expect the calibrated model to identify  $v_0$  well. The experiments are consistent with our expectation—from Table I, we can see the identified  $v_0$  varies in a large range for disparate models; and from Fig. 6 and Fig. 7, the posterior distributions of  $v_0$  are noisy and tend to larger  $v_0$ . However, experiments indicate that this heavily depends on whether the prior is strong enough—if we set a noninformative prior, the posterior would be unrealistically high; and if we set a very strong prior, it would be almost the same as our prior. Another interesting fact is that if we set a weak prior with a very large  $v_0$ , the model would still converge but with an unrealistic high posterior value of  $v_0$ ; the other parameters, however, are slightly changed.

## VI. SIMULATION

Based on the Bayesian calibration approach, in this section we propose a stochastic simulation method corresponding to the generative processes of the proposed Bayesian models, which is different from the traditional deterministic car-following simulations. Then, the quantitative analysis is demonstrated for comparison.

### A. Deterministic and Stochastic Simulations

Deterministic simulation is a commonly used approach in trajectory calibrations [7]. Typically, given the leading vehicle’s trajectory and the initial motion state of the following vehicle, we can use the calibrated IDM model to conduct simulations and obtain predicted motion states. Then, one can compare the predicted motion states with the observations to further help with either calibration or evaluation. In the previous literature, most motion states updating methods are based on Eq. (3), which is deterministic. Such deterministic simulations limit the simulator’s ability of reproducing anthropomorphic driving behaviors. Furthermore, as we elaborated in Section IV-B, only biased models would be obtained without considering serial correlation and the deterministic simulations are no exception.

Given that the intrinsic nature of our Bayesian model is probabilistic distribution, taking benefit from it, we propose a stochastic simulation method. The key idea is to sample an action  $a_d^{(t)}$  from Eq. (9) for the B-IDM or Eq. (13) for the MA-IDM instead of using a deterministic  $a_{\text{IDM } d}^{(t)}$ . The stochasticity of such simulation is determined by the noise level  $\sigma_\epsilon$ , calibrated from the data as discussed in Section V-B3. According to the parameter identification results in Table I, we control the noise level in simulations by fixing  $\sigma_\epsilon = 0.3 \text{ m/s}^2$  for the B-IDM and  $\sigma_\epsilon = 0.1 \text{ m/s}^2$  for the MA-IDM.

### B. Parameters Generation and Error Analysis for Deterministic Simulations

It was reported in the previous literature that car-following parameters simply drawn from uncorrelated marginal distributions could yield unreliable results in simulation and, consequently, inaccurate interpretation [37]. Here we emphasize that one advantage of our Bayesian method compared with the traditional optimization-based solution is obtaining the joint distributions of parameters instead of point estimations. Therefore, rather than using the expectation values from Table I, one can draw enormous samples from the joint posterior distributions to generate anthropomorphic driving behaviors. Specifically, from the viewpoint of a generative process, it is not difficult to sample  $\theta_d, d = 1, \dots, D$  from the posteriors of  $\theta$  (at the population level) to obtain disparate individual driving styles; and sample style-specific IDM parameters  $\theta_{d,i}, i = 1, \dots, N$  from the posteriors of  $\theta_d$  (at the individual level) to obtain enormous but nonidentical driving behaviors.

To evaluate the calibration and generation results, we use one representative driver for each vehicle type, i.e., the car driver #355 and the truck driver #211. We generate  $N = 5000$  sets of IDM parameters for each model. Then, by providing the leading vehicle’s trajectories and starting the followers with

TABLE II  
EVALUATIONS OF THE DETERMINISTIC AND STOCHASTIC SIMULATION RESULTS WITH DIFFERENT PROPOSED MODELS.

Data \ Model		Pooled model		Hierarchical model		Unpooled model	
		B-IDM	MA-IDM	B-IDM	MA-IDM	B-IDM	MA-IDM
Car #355	$e(a) \times 10$	$3.93 \pm 0.02$	$4.13 \pm 0.02$	$3.37 \pm 0.05$	<b><math>3.30 \pm 0.06</math></b>	$3.37 \pm 0.03$	$3.33 \pm 0.04$
	$e(v) \times 10$	$8.57 \pm 0.17$	$10.98 \pm 0.26$	$4.82 \pm 0.12$	<b><math>4.69 \pm 0.13</math></b>	$4.77 \pm 0.06$	$4.74 \pm 0.10$
	$e(s)$	$3.02 \pm 0.09$	$4.26 \pm 0.20$	$1.39 \pm 0.07$	<b><math>1.30 \pm 0.06</math></b>	$1.37 \pm 0.04$	$1.32 \pm 0.05$
	CRPS( $a$ )	0.23/0.54	0.25/0.55	<b>0.19/0.51</b>	<b>0.19/0.52</b>	<b>0.19/0.51</b>	0.20/ <b>0.51</b>
	CRPS( $v$ )	0.59/0.58	0.60/0.89	0.32/0.36	<b>0.26/0.27</b>	0.33/0.32	0.27/ <b>0.26</b>
	CRPS( $s$ )	2.21/4.74	2.59/5.85	0.89/3.32	<b>0.72/2.79</b>	0.90/3.18	0.76/ <b>2.73</b>
Truck #211	$e(a) \times 10$	$2.69 \pm 0.02$	$2.54 \pm 0.03$	$2.14 \pm 0.17$	<b><math>1.93 \pm 0.09</math></b>	$2.00 \pm 0.06$	<b><math>1.93 \pm 0.05</math></b>
	$e(v) \times 10$	$9.06 \pm 0.10$	$8.76 \pm 0.13$	$6.28 \pm 1.53$	$4.58 \pm 0.57$	$4.87 \pm 0.39$	<b><math>4.31 \pm 0.26</math></b>
	$e(s)$	$5.71 \pm 0.06$	$5.49 \pm 0.09$	$4.96 \pm 1.95$	$2.58 \pm 0.84$	$3.09 \pm 0.50$	<b><math>2.12 \pm 0.42</math></b>
	CRPS( $a$ )	0.15/0.07	0.13/0.06	0.12/0.07	<b>0.11/0.06</b>	0.12/0.07	<b>0.11/0.05</b>
	CRPS( $v$ )	0.75/1.47	0.56/0.92	0.37/0.22	<b>0.25/0.17</b>	0.33/0.08	<b>0.24/0.17</b>
	CRPS( $s$ )	4.53/2.56	3.64/1.29	2.64/7.72	1.31/3.91	1.83/6.07	<b>1.14/3.41</b>

the same initial conditions, we simulate the trajectories of the followers, whose behaviors are controlled by a calibrated IDM with a set of sampled parameters [38]. The simulation step is therefore set as 0.04sec which corresponds to the 25 Hz sampling frequency of the leading vehicle's data. To illustrate the simulated trajectories, we show the results with parameter samples from  $\theta_{\#211}$  in the top row of Fig. 8. In the following, we compare the ground-truth trajectories with the fully simulated trajectories via measuring the absolute root mean square errors (RMSE)  $e$  on their motion states (i.e.,  $a$ ,  $v$ , and  $s$ ), written as

$$e(x, \hat{\mathbf{f}}, \theta_{d,i}) = \sqrt{\frac{1}{N} \sum_{i=1}^N \left( f(x_i | \theta_{d,i}) - \hat{f}_i \right)^2}. \quad (16)$$

The simulation errors are reported in Table II in the form of (mean  $\pm$  standard deviation), where the models with the lowest error are bolded. Recall that the pooled models, acting as general behavioral models, were trained to fit all the car-following data of several drivers. Apparently, given that different drivers have distinct driving styles and have experienced dissimilar driving situations, the data could reflect diverse operating characteristics. Thus, a model that best fits a particular driver does not necessarily do so for a different driver [34]. Therefore, it is reasonable that the pooled models have limited performances. Besides, the simulation results indicate that the errors of the hierarchical models are at the same level as the unpooled models, which agrees with the findings in Section V-B2 that the hierarchical models can identify disparate IDM parameters of diverse drivers. Furthermore, although we can only obtain biased results in deterministic simulations, the results of the hierarchical models and the unpooled models still demonstrate that the MA-IDM has lower simulation errors than the B-IDM. As shown in Fig. 8, the predicted motion states with the calibrated MA-IDM tend to be closer to ground truth when compared with those driven by the calibrated B-IDM. These evidences support that considering serial correlations during parameter identification can reduce bias. However, it is worth noting that even though the identified parameters are unbiased since we considered the serial correlation during calibration,

the predicted motion states are still biased in deterministic simulations.

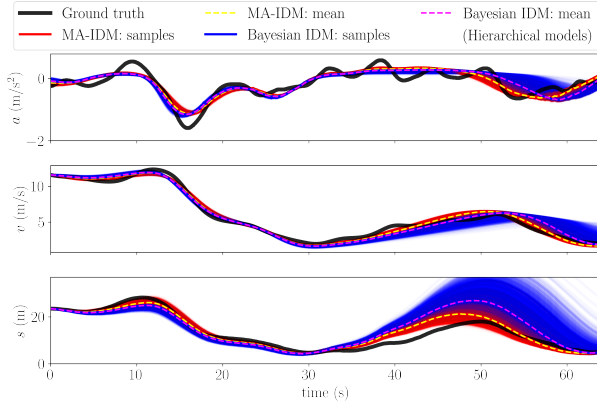
### C. Unbiased Estimation and Bayesian Evaluations for Stochastic Simulations

Benefiting from the Bayesian method, we can obtain posterior motion states in stochastic simulations rather than the predicted motion states in deterministic simulations. Here we propose a memory-augmented method by considering the serial correlation in stochastic simulations to obtain unbiased posterior motion states. Specifically, recall that we assumed  $a_d^{(t)} = a_{\text{IDM } d}^{(t)} + a_{\text{GP } d}^{(t)} + \epsilon$  in Section IV-B, we simulate the motion of the following vehicle at a certain timestamp by simultaneously taking several independent steps as follows. To initialize, we draw several random functions  $a_{\text{GP } d}$ ,  $d = 1, \dots, D$  from GP with the RBF kernel parameterized by  $\sigma_k = 0.2 \text{ m/s}^2$  and  $\ell = 33 \text{ s}$  at the beginning of the simulations. Then for each driver  $d$  at timestamp  $t$ : (1) we obtain the first term  $a_{\text{IDM } d}^{(t)}$  from IDM with the typical procedures in deterministic simulations; (2) we evaluate the  $d$ -th drawn function  $a_{\text{GP } d}^{(t)}$  at time  $t$  as the second term; (3) we sample a random noise  $\epsilon$  from  $\mathcal{N}(0, \sigma_\epsilon^2)$ . The posterior motion states are shown in the bottom row of Fig. 8.

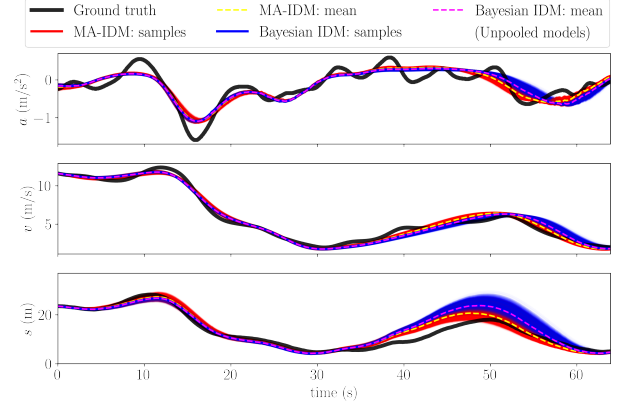
To evaluate the performances of stochastic simulations and quantify the uncertainty of posterior motion states, we adopted continuous ranked probability score (CRPS) [39], which can be written as

$$\text{CRPS}(y_t) = \int_{-\infty}^{+\infty} (F(y) - \mathbb{1}\{y > y_t\})^2 dy, \quad (17)$$

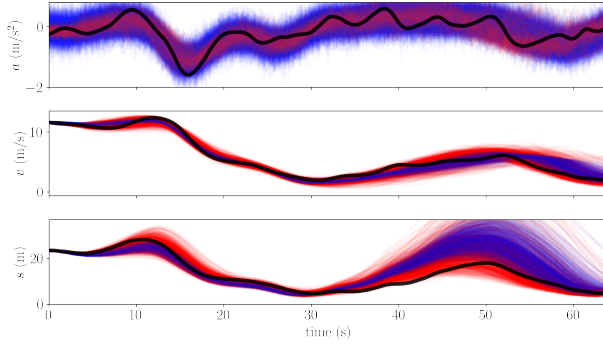
where  $y_t$  is the observation at time  $t$ ,  $F$  is the forecast cumulative distribution function, and  $\mathbb{1}$  is the indicator function. To build the evaluation metric, we first evaluate CRPS for  $a$ ,  $v$ , and  $s$  at each timestamp  $t$ , then averaging over time by  $\overline{\text{CRPS}}(y) = \frac{1}{T} \sum_{t=1}^T \text{CRPS}(y_t)$ . By noticing the gaps between the biased motion state predictions and the ground truth from the top row of Fig. 8, we also evaluate CRPS at  $t_0 = 37 \text{ s}$  and  $t_0 = 45 \text{ s}$  for car and truck data, respectively. The Bayesian evaluation results are shown in the form of  $(\overline{\text{CRPS}}(y)/\text{CRPS}(y_t|t=t_0))$  in Table II.



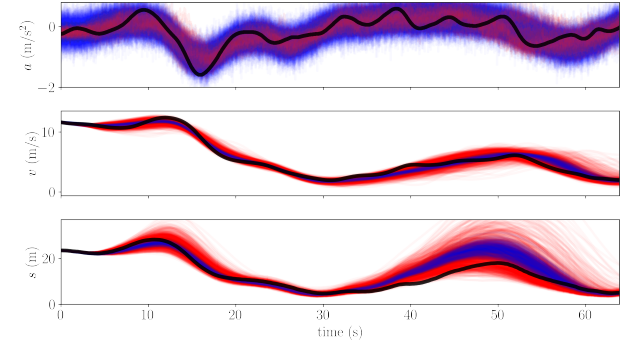
(a) Predicted motion states with hierarchical models.



(b) Predicted motion states with unpooled models.



(c) Posterior motion states with hierarchical models.



(d) Posterior motion states with unpooled models.

Fig. 8. The deterministic (top) and stochastic (bottom) simulation results of a representative truck driver #211. The black lines indicate the ground truth of human driving data; The yellow and fuchsia dotted lines are the predicted motion states with the expectations of parameter posteriors; The red and blue lines are the predicted motion states with the parameter samples drawn from posteriors.

From Fig. 8, an interesting but not surprising finding is the red lines in the bottom row (i.e., the posterior motion states of the MA-IDM) perfectly fix the gaps of predicted motion states shown in the top row. And the posterior motion states in unbiased simulations tightly contain the ground truth in the envelope. In addition, in stochastic simulations, although the B-IDM (the blue lines) loosely and easily contains the ground truth of the acceleration curve in its envelope, the simulated results for  $v$  and  $s$  are still biased. From Table II, we can conclude that CRPS is lowered in the memory-augmented simulations. Therefore, by introducing the memory-augmented method to model the serial correlation, the unbiased stochastic simulations with the unbiased parameters identified by the MA-IDM outperform the biased results in the B-IDM.

#### D. Multi-Vehicle Simulations in A Ring Scenario

The single-lane ring road network has been extensively studied to investigate the microscopic car-following behaviors in a closed traffic system [40], [41]. Several key elements determine the dynamics on the ring road: The ring radius is set as 128 m, which results in approximately 804 m of the circumference; The initial speed of each vehicle is set as 11.6 m/s; There are a total of 37 vehicles simulated for 3000 sec; The simulation step is set as 0.5 sec.

Here we conduct stochastic simulations with two different settings to compare the microscopic behaviors, as shown in Fig. 9. The left of Fig. 9 is simulated with homogeneous IDM parameters taken as the recommended values listed in Table I, and the noise level is controlled to the same level discussed in Section VI-A. The right part shows the results of the memory-augmented simulations, in which the GP settings are the same as in Section VI-C. As can be seen, we can observe a recurring pattern from the simulations with fixed IDM parameters, although a stochastic term is introduced. On the contrary, we can obtain different random car-following behaviors in the heterogeneous setting, which reflects the dynamic and diverse driving styles of different drivers. Additionally, we demonstrated the speed-density and flow-density fundamental diagrams of the simulation results, as shown in Fig. 10. These diagrams indicate that the simulations with heterogeneous IDM parameters can generate a wide variety of car-following behaviors, thus, are more realistic and stochastic than those with homogeneous ones.

### VII. FUTURE SCOPE AND DISCUSSIONS

#### A. Future Works

There are several aspects that can be further explored in future works. First, our method is not limited to calibrating

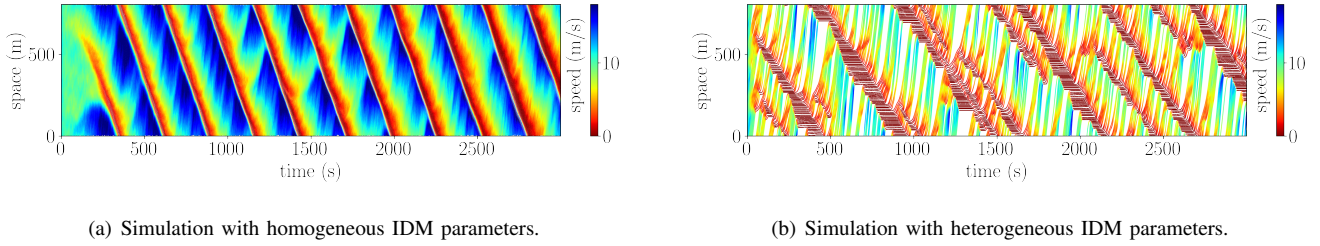


Fig. 9. Time-space diagram of multi-vehicle car-following simulations. (a) the parameters are taken as the recommendation values [19]. (b) the parameters are sampled from the posteriors in the hierarchical MA-IDM.

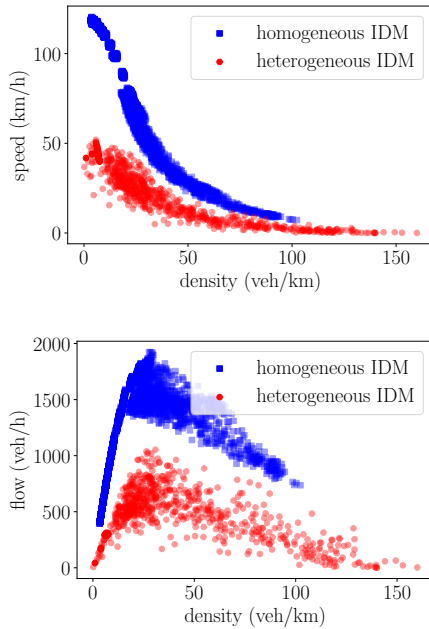


Fig. 10. Fundamental diagrams of ring-road simulation.

IDM; one can easily extend it to other microscopic car-following models (even other regression problems, see e.g., [42]) using a similar Bayesian scheme introduced in this work. Besides, the MoP is not restricted to using speed, as mentioned by [2]. Although the likelihood here is developed based on speed, the spacing or acceleration could also be a good MoP. One can easily make minor adjustments based on our method to calibrate car-following models using spacing or acceleration.

Additionally, human drivers have personalized styles, which are not life-long determined but time-varying [43]; thus, we ask: “how to model the dynamic time-varying IDM parameters for every single driver?” Following this concern, we further emphasize that in reality the residual variance and lengthscale should be scenario specific. For instance, one could freely take actions with a significant variance in free flow, but most drivers take almost the same actions (e.g., hard brake) in some risky scenarios. Thus, the GP hyperparameters (e.g., noise variance and temporal lengthscale) should be input-dependent, and the GP itself will become nonstationary. An interesting research question is to quantify how the GP hyperparameters vary with

the input/scenario using non-stationary GP regression [44].

Furthermore, more realistic scenarios involving multiple factors can be studied by extending our model into a more complex architecture. For instance, human driving behaviors result from frequent transitions among various driving styles [43], [45]. Thus, it is no longer reasonable to model the driving behaviors using a single distribution; instead, a mixture model is suitable [46]. In addition, as mentioned in [47], power dynamics of vehicle are not uniform across the speed range; also, different vehicles (e.g., cars and trucks in this work) have differences in power capabilities. These factors lead to vehicle dynamics heterogeneity [47], [48], which can be modeled by constructing deeper hierarchical models, e.g., add another layer in Fig.3 to depict different vehicle dynamic characteristics.

### B. Open Discussions

Here we post some open questions to be discussed with the community. Although we have calibrated an unpooled model, we note that the calibration results will not be so satisfactory since the segment is too short and contains minimal information (e.g., with only congestion but without high-speed free flow data, or vice versa.) So, we must reconsider when collecting data:

- What kinds of data are preferable for calibrating an accurate car-following model? Which maneuvers (e.g., free-flow, freely accelerating, approaching, keeping distance, etc.) that are missing in the training data may significantly impact the calibration performance? Is the model calibrated on data with partial maneuvers meaningful? If so, how to evaluate the calibration performance in the scenarios of the missing maneuvers?

These questions further lead us to the discussion about the data collection methods. By leveraging different methods and sensors, a lot of microscopic datasets are constructed. For instance, sensor data collected by stationary loop detectors, extended floating-car data (xFCD) collected by GPS, trajectory data collected by drone, etc. Limitations are obvious for each data collection method: stationary loop detectors are mounted on the road, thus can only obtain information at a specific location; xFCD care more about ego vehicle’s motion states but only with limited information regarding other traffic participants; drones collect data based computer vision approach, which can only extract trajectory from a limited ROI<sup>2</sup>.

<sup>2</sup>The pNEUMA dataset [49] is a great attempt trying to extend the ROI by sharing information among a swarm of drones.

In the near future of Internet of Things (IoT) for transportation, we still wondering:

- How to collect high-quality public-available datasets with rich information? How to leverage different data collection methods with IoT for transportation? Whose data should we use/trust when obtaining different values from different sensors regarding the same variable?

Additionally, Gaussian processes still have some limitations. For instance, as we mentioned in Section V-C—when data is limited, setting a strong prior would constraint the posterior near to our prior; but setting a noninformative prior would have unrealistic results. Also, the computational complexity has limited its application to larger datasets.

- How to select an appropriate prior in Bayesian methods? How to construct the kernel function that suits the driving characteristics? How to compare and incorporate different stochastic processes to modeling driving behaviors?

### VIII. CONCLUSION

Most literature developed their models upon the i.i.d. assumption of residuals, which does not hold. This paper developed a novel car-following model (i.e., the MA-IDM) by leveraging Bayesian methods and Gaussian processes, which model the serial correlation of residuals. In such a way, it makes the i.i.d. assumption valid and has the model calibration unbiased. Extensive experiments compare the pooled, hierarchical, and unpooled models for both of the B-IDM and the MA-IDM. Experiment results demonstrate the effectiveness of the MA-IDM. With the well-calibrated MA-IDM, we also developed an unbiased stochastic simulator, which generates enormous drivers with nonidentical driving behaviors, and provides insight into creating a realistic simulator.

### REFERENCES

- [1] I. D. Ofiteru and C. Picioreanu, “No model is perfect, but some are useful,” *Science*, vol. 376, no. 6596, pp. 914–916, 2022.
- [2] V. Punzo, Z. Zheng, and M. Montanino, “About calibration of car-following dynamics of automated and human-driven vehicles: Methodology, guidelines and codes,” *Transportation Research Part C: Emerging Technologies*, vol. 128, p. 103165, 2021.
- [3] S. Hoogendoorn and R. Hoogendoorn, “Calibration of microscopic traffic-flow models using multiple data sources,” *Philosophical Transactions of the Royal Society A: Mathematical, Physical and Engineering Sciences*, vol. 368, no. 1928, pp. 4497–4517, 2010.
- [4] M. Rahman, M. Chowdhury, T. Khan, and P. Bhavsar, “Improving the efficacy of car-following models with a new stochastic parameter estimation and calibration method,” *IEEE Transactions on Intelligent Transportation Systems*, vol. 16, no. 5, pp. 2687–2699, 2015.
- [5] F. Abodo, A. Berthume, S. Zitzow-Childs, and L. Bobadilla, “Strengthening the case for a bayesian approach to car-following model calibration and validation using probabilistic programming,” in *2019 IEEE Intelligent Transportation Systems Conference (ITSC)*. IEEE, 2019, pp. 4360–4367.
- [6] X. Wang, R. Jiang, L. Li, Y. Lin, X. Zheng, and F.-Y. Wang, “Capturing car-following behaviors by deep learning,” *IEEE Transactions on Intelligent Transportation Systems*, vol. 19, no. 3, pp. 910–920, 2017.
- [7] M. Treiber and A. Kesting, “Microscopic calibration and validation of car-following models—a systematic approach,” *Procedia-Social and Behavioral Sciences*, vol. 80, pp. 922–939, 2013.
- [8] V. Punzo and M. Montanino, “A two-level probabilistic approach for validation of stochastic traffic simulations: impact of drivers’ heterogeneity models,” *Transportation research part C: emerging technologies*, vol. 121, p. 102843, 2020.
- [9] D. Cochran and G. H. Orcutt, “Application of least squares regression to relationships containing auto-correlated error terms,” *Journal of the American statistical association*, vol. 44, no. 245, pp. 32–61, 1949.
- [10] M. Treiber and A. Kesting, “Traffic flow dynamics,” *Traffic Flow Dynamics: Data, Models and Simulation*, Springer-Verlag Berlin Heidelberg, pp. 983–1000, 2013.
- [11] R. Krajewski, J. Bock, L. Kloecker, and L. Eckstein, “The highd dataset: A drone dataset of naturalistic vehicle trajectories on german highways for validation of highly automated driving systems,” in *2018 21st International Conference on Intelligent Transportation Systems (ITSC)*, 2018, pp. 2118–2125.
- [12] M. C. Kennedy and A. O’Hagan, “Bayesian calibration of computer models,” *Journal of the Royal Statistical Society: Series B (Statistical Methodology)*, vol. 63, no. 3, pp. 425–464, 2001.
- [13] C. Chen, L. Li, J. Hu, and C. Geng, “Calibration of mitsim and idm car-following model based on ngsim trajectory datasets,” in *Proceedings of 2010 IEEE International Conference on Vehicular Electronics and Safety*. IEEE, 2010, pp. 48–53.
- [14] S. P. Hoogendoorn and S. Ossen, “Parameter estimation and analysis of car-following models,” in *Transportation and Traffic Theory. Flow, Dynamics and Human Interaction. 16th International Symposium on Transportation and Traffic Theory* University of Maryland, College Park, 2005.
- [15] J. Durbin and G. S. Watson, “Testing for serial correlation in least squares regression: I,” *Biometrika*, vol. 37, no. 3/4, pp. 409–428, 1950.
- [16] G. Welch, G. Bishop, et al., “An introduction to the kalman filter,” 1995.
- [17] R. J. Hyndman and G. Athanasopoulos, *Forecasting: principles and practice*. OTexts, 2018.
- [18] C. E. Rasmussen, “Gaussian processes in machine learning,” in *Summer school on machine learning*. Springer, 2003, pp. 63–71.
- [19] M. Treiber, A. Hennecke, and D. Helbing, “Congested traffic states in empirical observations and microscopic simulations,” *Physical review E*, vol. 62, no. 2, p. 1805, 2000.
- [20] M. Treiber, A. Kesting, and D. Helbing, “Delays, inaccuracies and anticipation in microscopic traffic models,” *Physica A: Statistical Mechanics and its Applications*, vol. 360, no. 1, pp. 71–88, 2006.
- [21] R. P. Bhattacharyya, R. Senanayake, K. Brown, and M. J. Kochenderfer, “Online parameter estimation for human driver behavior prediction,” in *2020 American Control Conference (ACC)*. IEEE, 2020, pp. 301–306.
- [22] M. Treiber and A. Kesting, “The intelligent driver model with stochasticity—new insights into traffic flow oscillations,” *Transportation research procedia*, vol. 23, pp. 174–187, 2017.
- [23] A. Gelman, “Multilevel (hierarchical) modeling: what it can and cannot do,” *Technometrics*, vol. 48, no. 3, pp. 432–435, 2006.
- [24] D. Lewandowski, D. Kurowicka, and H. Joe, “Generating random correlation matrices based on vines and extended onion method,” *Journal of multivariate analysis*, vol. 100, no. 9, pp. 1989–2001, 2009.
- [25] J. Salvatier, T. V. Wiecki, and C. Fonnesbeck, “Probabilistic programming in python using pymc3,” *PeerJ Computer Science*, vol. 2, p. e55, 2016.
- [26] I. Alvarez, J. Niemi, and M. Simpson, “Bayesian inference for a covariance matrix,” *arXiv preprint arXiv:1408.4050*, 2014.
- [27] M. Montanino and V. Punzo, “Trajectory data reconstruction and simulation-based validation against macroscopic traffic patterns,” *Transportation Research Part B: Methodological*, vol. 80, pp. 82–106, 2015.
- [28] V. Punzo, M. T. Borzacchiello, and B. Ciuffo, “On the assessment of vehicle trajectory data accuracy and application to the next generation simulation (ngsim) program data,” *Transportation Research Part C: Emerging Technologies*, vol. 19, no. 6, pp. 1243–1262, 2011.
- [29] C. Zhang, J. Zhu, W. Wang, and J. Xi, “Spatiotemporal learning of multivehicle interaction patterns in lane-change scenarios,” *IEEE Transactions on Intelligent Transportation Systems*, 2021.
- [30] V. Punzo, M. Montanino, and B. Ciuffo, “Do we really need to calibrate all the parameters? variance-based sensitivity analysis to simplify microscopic traffic flow models,” *IEEE Transactions on Intelligent Transportation Systems*, vol. 16, no. 1, pp. 184–193, 2014.
- [31] L. Liu, L. Zhu, and D. Yang, “Modeling and simulation of the car-truck heterogeneous traffic flow based on a nonlinear car-following model,” *Applied Mathematics and Computation*, vol. 273, pp. 706–717, 2016.
- [32] M. D. Hoffman, A. Gelman, et al., “The no-u-turn sampler: adaptively setting path lengths in hamiltonian monte carlo,” *J. Mach. Learn. Res.*, vol. 15, no. 1, pp. 1593–1623, 2014.
- [33] D. Foreman-Mackey, “corner.py: Scatterplot matrices in python,” *The Journal of Open Source Software*, vol. 1, no. 2, p. 24, jun 2016. [Online]. Available: <https://doi.org/10.21105/joss.00024>
- [34] A. Kesting and M. Treiber, “Calibrating car-following models by using trajectory data: Methodological study,” *Transportation Research Record*, vol. 2088, no. 1, pp. 148–156, 2008.
- [35] T. J. Triggs, W. G. Harris, et al., “Reaction time of drivers to road stimuli,” 1982.

- [36] Y. Wang, M. L. Delle Monache, and D. B. Work, "Identifiability of car-following dynamics," *Physica D: Nonlinear Phenomena*, vol. 430, p. 133090, 2022.
- [37] J. Kim and H. S. Mahmassani, "Correlated parameters in driving behavior models: Car-following example and implications for traffic microsimulation," *Transportation Research Record*, vol. 2249, no. 1, pp. 62–77, 2011.
- [38] B. Ciuffo, V. Punzo, and V. Torrieri, "Comparison of simulation-based and model-based calibrations of traffic-flow microsimulation models," *Transportation Research Record*, vol. 2088, no. 1, pp. 36–44, 2008.
- [39] J. E. Matheson and R. L. Winkler, "Scoring rules for continuous probability distributions," *Management science*, vol. 22, no. 10, pp. 1087–1096, 1976.
- [40] M. Treiber and A. Kesting, "An open-source microscopic traffic simulator," *IEEE Intelligent Transportation Systems Magazine*, vol. 2, no. 3, pp. 6–13, 2010.
- [41] Y. Sugiyama, M. Fukui, M. Kikuchi, K. Hasebe, A. Nakayama, K. Nishinari, S.-i. Tadaki, and S. Yukawa, "Traffic jams without bottlenecks—experimental evidence for the physical mechanism of the formation of a jam," *New journal of physics*, vol. 10, no. 3, p. 033001, 2008.
- [42] Z. Cheng, X. Wang, X. Chen, M. Trepanier, and L. Sun, "Bayesian calibration of traffic flow fundamental diagrams using gaussian processes," *arXiv preprint arXiv:2208.02799*, 2022.
- [43] J. Yarlagadda and D. S. Pawar, "Heterogeneity in the driver behavior: an exploratory study using real-time driving data," *Journal of advanced transportation*, vol. 2022, 2022.
- [44] M. Heinonen, H. Mannerström, J. Rousu, S. Kaski, and H. Lähdesmäki, "Non-stationary gaussian process regression with hamiltonian monte carlo," in *Artificial Intelligence and Statistics*. PMLR, 2016, pp. 732–740.
- [45] W. Wang, J. Xi, and D. Zhao, "Driving style analysis using primitive driving patterns with bayesian nonparametric approaches," *IEEE Transactions on Intelligent Transportation Systems*, vol. 20, no. 8, pp. 2986–2998, 2018.
- [46] —, "Learning and inferring a driver's braking action in car-following scenarios," *IEEE Transactions on Vehicular Technology*, vol. 67, no. 5, pp. 3887–3899, 2018.
- [47] M. A. Makridis, A. Anesiadou, K. Mattas, G. Fontaras, and B. Ciuffo, "Characterising driver heterogeneity within stochastic traffic simulation," *Transportmetrica B: Transport Dynamics*, vol. 0, no. 0, pp. 1–19, 2022.
- [48] B. Ciuffo, M. Makridis, T. Toledo, and G. Fontaras, "Capability of current car-following models to reproduce vehicle free-flow acceleration dynamics," *IEEE Transactions on Intelligent Transportation Systems*, vol. 19, no. 11, pp. 3594–3603, 2018.
- [49] E. Barmounakis and N. Geroliminis, "On the new era of urban traffic monitoring with massive drone data: The pneuma large-scale field experiment," *Transportation research part C: emerging technologies*, vol. 111, pp. 50–71, 2020.



**Lijun Sun** (Senior Member, IEEE) received the B.S. degree in civil engineering from Tsinghua University, Beijing, China, in 2011, and the Ph.D. degree in civil engineering (transportation) from the National the University of Singapore in 2015. He is currently an Assistant Professor in the Department of Civil Engineering, McGill University, Montreal, QC, Canada. His research centers on intelligent transportation systems, machine learning, spatiotemporal modeling, travel behavior, and agent-based simulation.



**Chengyuan Zhang** (Student Member, IEEE) is a Ph.D. student with the Department of Civil Engineering, McGill University. He received his B.S. degree in Automotive Engineering from Chongqing University, Chongqing, China, in 2019. From 2019 to 2020, he worked as a visiting researcher with the Department of Mechanical Engineering, UC Berkeley. His research interests are Bayesian learning, macro/micro human driving behavior analysis, and multi-agent interaction modeling in intelligent transportation systems.